

NMCP/97-17
hep-lat/9801009

Confinement Artifacts in the $U(1)$ and $SU(2)$ Compact Lattice Gauge Theories*

Kevin Cahill[†] and Gary Herling[‡]

New Mexico Center for Particle Physics
University of New Mexico
Albuquerque, NM 87131-1156

Abstract

We identify the artifact that causes confinement at strong coupling in compact $U(1)$ lattice gauge theory and show that more than 90% of the string tension in compact $SU(2)$ lattice gauge theory is due to plaquettes of negative trace.

April 2, 2019

*Research supported by the U.S. Department of Energy

[†]kevin@cahill.phys.unm.edu <http://cahill.phys.unm.edu/kevin>

[‡]Member of the Center for Advanced Studies; e-mail: herling@unm.edu

1 Introduction

We report here the results of two studies of lattice artifacts. The first study shows that compact $U(1)$ gauge theory displays confinement at strong coupling because its links are circles. One may remove this artifact by using a thin barrier to cut the circle.

The second study shows that most of the confinement signal in compact $SU(2)$ gauge theory is due to plaquettes of negative trace and that, when such plaquettes are avoided, the ratio σ/Λ_L^2 is only about 1.6 ± 0.2 as opposed to about 31 ± 4 when they are included. Since the avoidance of plaquettes of negative trace is unlikely to affect perturbative quantities, the decrease in σ/Λ_L^2 may be attributed to a decrease in the string tension σ . Hence more than 90% of the confinement signal in compact lattice gauge theory is due to plaquettes of negative trace.

2 Why Compact $U(1)$ Confines

Compact lattice simulations of $U(1)$ gauge theory display confinement at strong coupling. In Figure 1 we plot the Creutz ratios[1] we obtained from simulations guided by the Wilson action and compare them with the exact values of free continuum QED indicated by the curves. At $\beta = 0.75$, the Creutz ratios $\chi(2,2)$, $\chi(2,3)$, $\chi(2,4)$, and $\chi(3,3)$ all overlap in a striking confinement signal. The Wilson action for $U(1)$ confines at strong coupling because the links

$$U(x, \mu) = \exp [i\theta(x, \mu)] = \exp [ieaA_\mu(x)] \quad (1)$$

take values on the unit circle.

One can avoid this artifact by placing a thin infinite barrier at $|\theta| = \pi$. We used a Metropolis algorithm and rejected any plaquette whose phase θ was either greater than $\pi - \epsilon$ or less than $-\pi + \epsilon$. We ran on a 12^4 lattice and began all runs from a cold start in which all links were unity. Our Creutz ratios display no sign of confinement and tend to follow the curves of the exact Creutz ratios of free continuum QED. The agreement with the exact ratios is better if ones uses an effective inverse coupling $\beta_e = \lambda^2\beta$ with

$\lambda^2 = 0.73$. In Figure 2 we plot the measured and exact Creutz ratios from $\beta = 0.25$ to $\beta = 1.5$. Although the continuum theory is free and exactly soluble, the lattice action is non-linear and does require renormalization. The renormalization $g_e = g_0/\lambda$ is the simplest rule that in the continuum limit satisfies

$$\lim_{g_0 \rightarrow 0} \frac{|g^2 - g_0^2|}{g_0} = 0. \quad (2)$$

We saw no confinement signal as long as the step size was smaller than the thickness 2ϵ of the cut in the phase θ . We took $.024 < \epsilon < 0.100$ and noticed no sensitivity to ϵ within that range. The nearly overlapping points at $\beta = 1.5$ correspond to $\epsilon = .024$ and to $\epsilon = 0.1$. We also performed simulations with Manton's action using $\epsilon = 0.026$ and found a similar absence of confinement.

Confinement signals arise when links are decorrelated. At strong coupling many $U(1)$ plaquettes are near -1 . Thus when a link on a plaquette that is near -1 is being updated, that link can jump to a value (often far from 1) that pushes the plaquette past the point -1 of maximum action to a lower action. After many such events, the links are decorrelated, and a confinement signal appears.

One may also interpret these results in terms of monopoles [2]. When the phase θ of each plaquette is required to lie between $\pi - \epsilon$ and $-\pi + \epsilon$, it follows that for $\epsilon > 0$, no string can ever penetrate any plaquette.

3 Compact $SU(2)$

In view of these results for $U(1)$, one might wonder whether similar lattice artifacts exist in the case of the group $SU(2)$. Because $U(1)$ and $SU(2)$ have different first homotopy groups ($\pi_1(U(1)) = Z$ but $\pi_1(SU(2)) = 0$), it would seem likely that the excision of a small cap around the antipode ($g = -1$) on the $SU(2)$ group manifold (the three sphere S_3 in four dimensions) would have little effect upon the Creutz ratios.

To check this assumption, we ran from cold starts on an 8^4 lattice and used a Metropolis algorithm with a modified form of the Wilson action in which we rejected plaquettes that lay within a small cap around the antipode.

Specifically the allowed plaquettes P had to satisfy the rule

$$\frac{1}{2}\text{Tr}P > -\cos\left(\frac{\pi}{10}\right) \approx -0.951. \quad (3)$$

In terms of the parameterization

$$\exp\left(i\frac{\vec{\theta}}{2} \cdot \vec{\sigma}\right) = \cos\left(\frac{|\vec{\theta}|}{2}\right) I + i\hat{\theta} \cdot \vec{\sigma} \sin\left(\frac{|\vec{\theta}|}{2}\right), \quad (4)$$

the excluded cap is described by the condition

$$\frac{9\pi}{5} \leq |\vec{\theta}| \leq \frac{11\pi}{5}. \quad (5)$$

The step size was small compared to the size of the excluded cap. As expected, the Creutz ratios $\chi(i, j)$ do not depend upon whether the small cap was excluded. At $\beta = 2$, for example, the Creutz ratios with the cap included are: $\chi(2, 2) = 0.5995(1)$, $\chi(2, 3) = 0.5813(4)$, $\chi(2, 4) = 0.582(5)$, $\chi(3, 3) = 0.556(5)$, and $\chi(3, 4) = 0.54(2)$; while with the cap excluded they are: $\chi(2, 2) = 0.596(3)$, $\chi(2, 3) = 0.570(8)$, $\chi(2, 4) = 0.55(2)$, $\chi(3, 3) = 0.46(5)$, and $\chi(3, 4) = 0.5(1)$. The exclusion of the cap makes little difference.

But what about the excision of a large cap? To study this question, we performed simulations using a Metropolis algorithm and a modified form of the Wilson action in which we rejected all plaquettes that had a negative trace, thus excluding half of the $SU(2)$ sphere. This positive-plaquette Wilson action has been studied by other groups [3]. We used an 8^4 lattice and began with all $SU(2)$ group elements equal to the identity (cold starts). We used a very small step size; the maximum change in any of the four real numbers that describe each group element was 0.005. Because of the small step size, we allowed 2,000,000 sweeps for thermalization.

In our positive-plaquette simulations, the Creutz ratios $\chi(i, j)$ as functions of β tend to follow the values given by the $SU(2)$ tree-level perturbative formula [4]

$$\chi_0(i, j, \beta) = \frac{3}{2\pi^2\beta} [-u(i, j) - u(i-1, j-1) + u(i, j-1) + u(i-1, j)] \quad (6)$$

where

$$u(i, j) = \frac{i}{j} \arctan \frac{i}{j} + \frac{j}{i} \arctan \frac{j}{i} - \log \left(\frac{1}{i^2} + \frac{1}{j^2} \right). \quad (7)$$

The fit of the perturbative formula to the data improves if we use an effective inverse coupling $\beta_e = \lambda^2 \beta$ which corresponds to a renormalized coupling constant $g = g_0/\lambda$ with $0 < \lambda \leq 1$. This scheme offers the simplest renormalization of the coupling constant that in the continuum limit satisfies the condition (2). In Figure 3 we plot the Creutz ratios $\chi(i, j)$ we obtained in simulations guided by the positive-plaquette Wilson action. The curves display the perturbative values as given by the tree-level formulas (6) and (7) with the effective inverse coupling $\beta_e = 0.54 \beta$. The data follow the perturbative curves near $\beta = 3$ but not near $\beta = 1$ where the bunching of the Creutz ratios for different i and j indicates confinement.

In the confining phase, the Creutz ratios $\chi(i, j)$ ought to be given approximately by the product of the string tension σ and the square of the lattice spacing $a^2(\beta_e)$. For the group $SU(2)$, the two-loop result for the dependence of this product $\sigma a^2(\beta_e)$ upon the effective inverse coupling β_e is

$$\sigma a^2(\beta_e) \approx \frac{\sigma}{\Lambda_L^2} \exp \left[-\frac{6\pi^2 \beta_e}{11} + \frac{102}{121} \log \left(\frac{6\pi^2 \beta_e}{11} \right) \right], \quad (8)$$

where Λ_L is the lattice scale parameter [1]. We expect this scaling formula to hold in a transition region where perturbation theory is still valid and where the quark-antiquark static potential $V(r)$ is a linear combination of a confining potential and a Coulomb potential:

$$\chi(i, j) = \frac{1}{(\beta_{\max} - \beta_{\min})} \left[(\beta_{\max} - \beta) \sigma a^2(\beta_e) + (\beta - \beta_{\min}) \chi_0(i, j, \beta_e) \right] \quad (9)$$

in which the string tension $\sigma a^2(\beta_e)$ is given by the scaling formula (8) and the perturbative Creutz ratio $\chi_0(i, j, \beta_e)$ is given by the tree-level formula (6–7). Near one end of this region, the potential $V(r)$ is mostly Coulomb; near the other end, $V(r)$ is mostly linear.

In simulations guided by the positive-plaquette Wilson action, we found a wide transition region between $\beta = 1.0$ and $\beta = 3.0$. Our best fit to the Creutz ratios $\chi(2, 2, \beta)$, $\chi(2, 3, \beta)$, $\chi(2, 4, \beta)$, and $\chi(3, 3, \beta)$ at $\beta = 1.0, 1.25, 1.5, 1.75, 2.0, 2.25, 2.5, 2.75$, and 3.0 was $\beta_e = 0.36 \beta$, $\beta_{\min} = -3.20$, $\beta_{\max} =$

6.75, and $\sigma_{PP}/\Lambda_L^2 = 1.58 \pm 0.2$. In the interpolation (9), the coefficient $(\beta_{\max} - \beta)/(\beta_{\max} - \beta_{\min})$ of the positive-plaquette string-tension term $\sigma_{PP}a^2(\beta_e)$ runs from 0.58 at $\beta = 1.0$ to 0.38 at $\beta = 3.0$, and the coefficient $(\beta - \beta_{\min})/(\beta_{\max} - \beta_{\min})$ of the tree-level perturbative term $\chi_0(i, j, \beta_e)$ runs from 0.42 at $\beta = 1.0$ to 0.62 at $\beta = 3.0$. Our fit to the data is displayed in Figure 4.

The ratio σ/Λ_L^2 of the string tension to the square of the lattice scale parameter is hard to measure accurately [5], and our procedure is subject to systematic errors due to our measurement scheme and to the small size of our lattice. To minimize these systematic errors, we applied the same procedure to the unmodified Wilson action and computed a ratio of ratios: the ratio σ_{PP}/Λ_L^2 divided by the ratio σ_W/Λ_L^2 in which σ_{PP} is the positive-plaquette string tension, σ_W is the Wilson string tension, and Λ_L is the lattice scale parameter.

We performed simulations of $SU(2)$ gauge theory guided by the unmodified Wilson action on an 8^4 lattice and measured the ratio σ_W/Λ_L^2 by the same procedure that we used to measure the positive-plaquette Wilson action. We found a narrow transition region between $\beta = 2.125$ and $\beta = 2.5$ in which our best fit was $\beta_e = 0.43\beta$, $\beta_{\min} = 1.42$, $\beta_{\max} = 2.64$, and $\sigma_W/\Lambda_L^2 = 30.8 \pm 4$. In the interpolation (9), the coefficient $(\beta_{\max} - \beta)/(\beta_{\max} - \beta_{\min})$ of the Wilson string-tension term $\sigma_W a^2(\beta_e)$ runs from 0.42 at $\beta = 2.125$ to 0.12 at $\beta = 2.5$, and the coefficient $(\beta - \beta_{\min})/(\beta_{\max} - \beta_{\min})$ of the tree-level perturbative term $\chi_0(i, j, \beta_e)$ runs from 0.58 at $\beta = 2.125$ to 0.88 at $\beta = 2.5$. Our fit is shown in Figure 5.

The rejection of the plaquettes of negative trace is generally regarded as an entirely non-perturbative modification of the Wilson action. To the extent that this is true, we may conclude that the value of the perturbative lattice parameter Λ_L appropriate to our modified version of Wilson's action is the same as that for the unmodified Wilson action. Thus our ratio of the positive-plaquette ratio $\sigma_{PP}/\Lambda_L^2 = 1.58 \pm 0.2$ to the Wilsonian ratio $\sigma_W/\Lambda_L^2 = 30.8 \pm 4$ may be identified as the ratio of the positive-plaquette string tension σ_{PP} to the Wilson string tension σ_W ,

$$\frac{\sigma_{PP}/\Lambda_L^2}{\sigma_W/\Lambda_L^2} = \frac{\sigma_{PP}}{\sigma_W} = 0.05. \quad (10)$$

We conclude that more than 90% of the confinement signal measured in

Wilsonian simulations is due to the plaquettes of negative trace, which are lattice artifacts.

Acknowledgments

We have benefited particularly from the perceptive advice of M. Creutz. We also are indebted to G. Marsaglia, W. Press, and J. Smit for useful conversations, to the Department of Energy for support under grant DE-FG03-92ER40732/B005, and to B. Dieterle, J. Barnes, and J. Sobolewski for the use of computers they control. Some of these computations were performed at NERSC.

References

- [1] M. Creutz, *Phys. Rev. D* 21 (1980) 2308; *Phys. Rev. Letters* 45 (1980) 313.
- [2] T. A. DeGrand and D. Toussaint, *Phys. Rev. D* 22 (1980) 2478.
- [3] G. Mack and E. Pietarinen, *Nucl. Phys.* B205 [FS5] (1982) 141; V. G. Bornyakov, M. Creutz and V. Mitryushkin, *Phys. Rev. D* 44 (1991) 3918; J. Ambjørn and G. Thorleifsson, *Phys. Rev. D* 50 (1994) 4715; and J. Fingberg, U. M. Heller, and V. Mitryushkin, *Nucl. Phys.* B435 (1995) 311.
- [4] K. Cahill, *Phys. Lett.* B304 (1993) 307.
- [5] F. Gutbrod, *Z. Phys. C* 30 (1986) 585, 37 (1987) 143, 55 (1992) 463; *Phys. Lett. B* 186 (1987) 389; B. A. Berg and A. H. Billoir, *Phys. Rev. D* 40 (1989) 550.

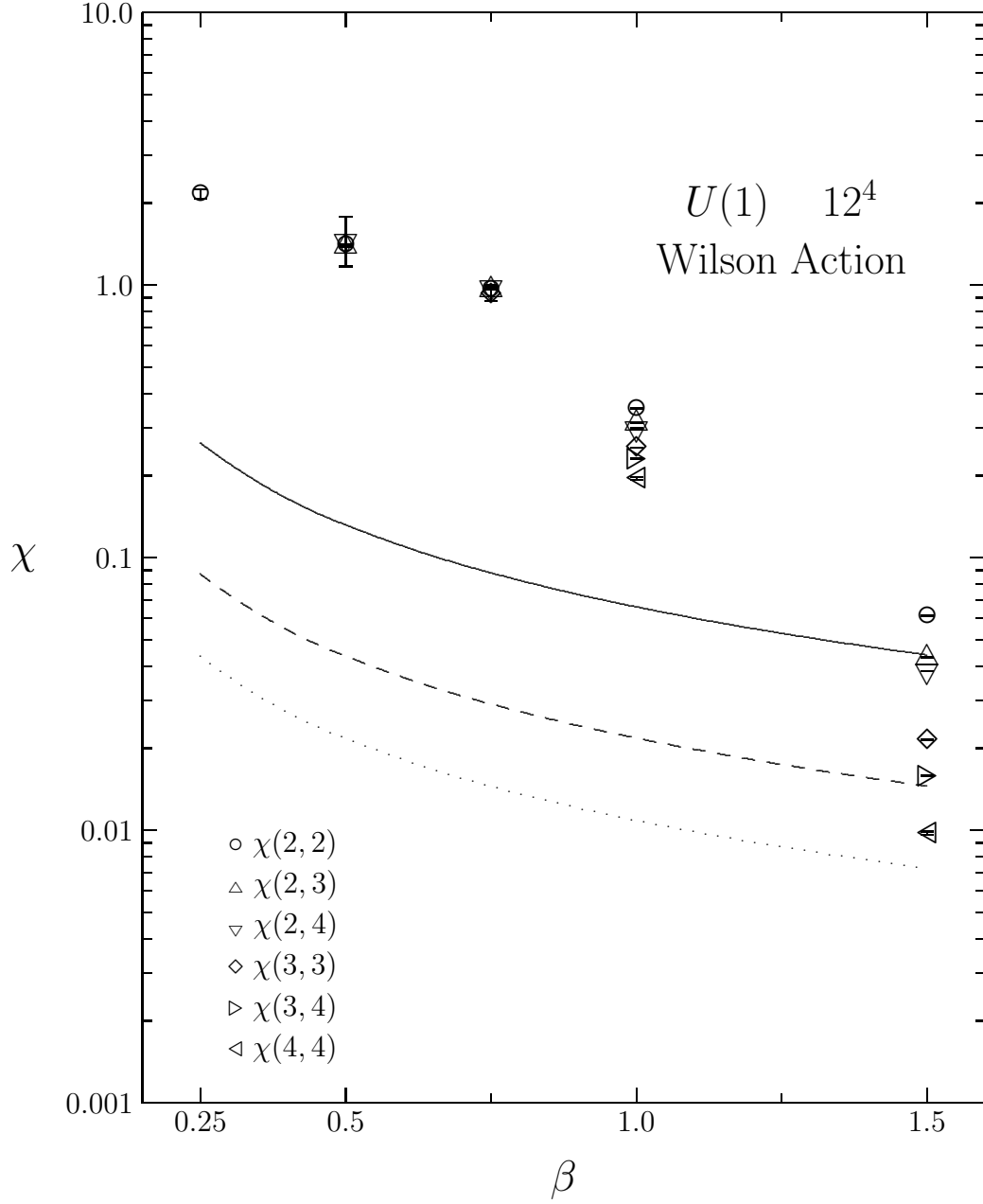


Figure 1: The $U(1)$ Creutz ratios $\chi(i, j)$ as given by Wilson's action and the exact Creutz ratios, $\chi(2, 2)$ (solid), $\chi(3, 3)$ (dashes), and $\chi(4, 4)$ (dots). The confinement signal at $\beta = 0.75$ is striking.

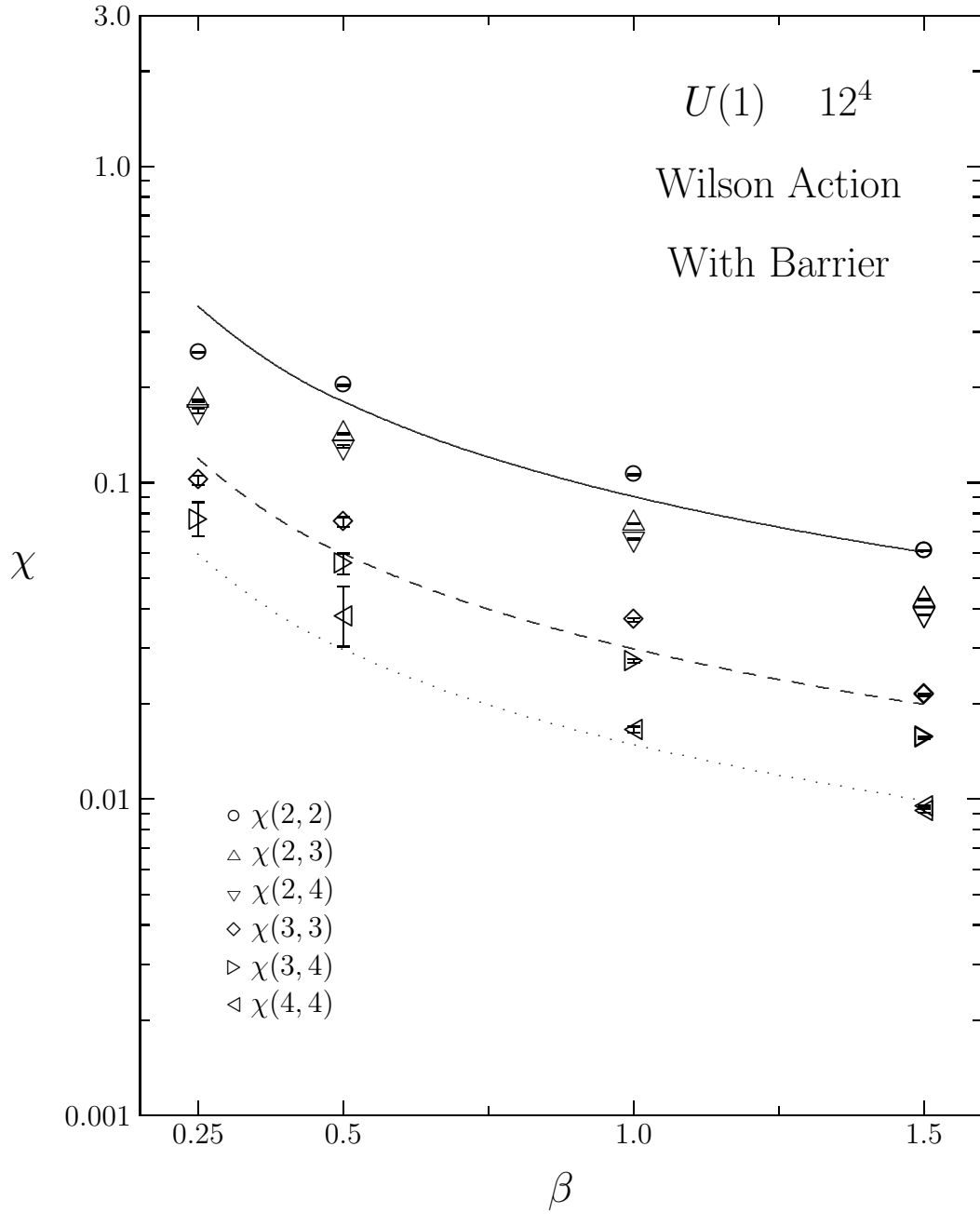


Figure 2: The $U(1)$ Creutz ratios $\chi(i, j)$, as given by Wilson's action with a small barrier, and the exact Creutz ratios at $\beta_e = 0.73 \beta$, $\chi(2, 2)$ (solid), $\chi(3, 3)$ (dashes), and $\chi(4, 4)$ (dots). There is no false confinement signal.

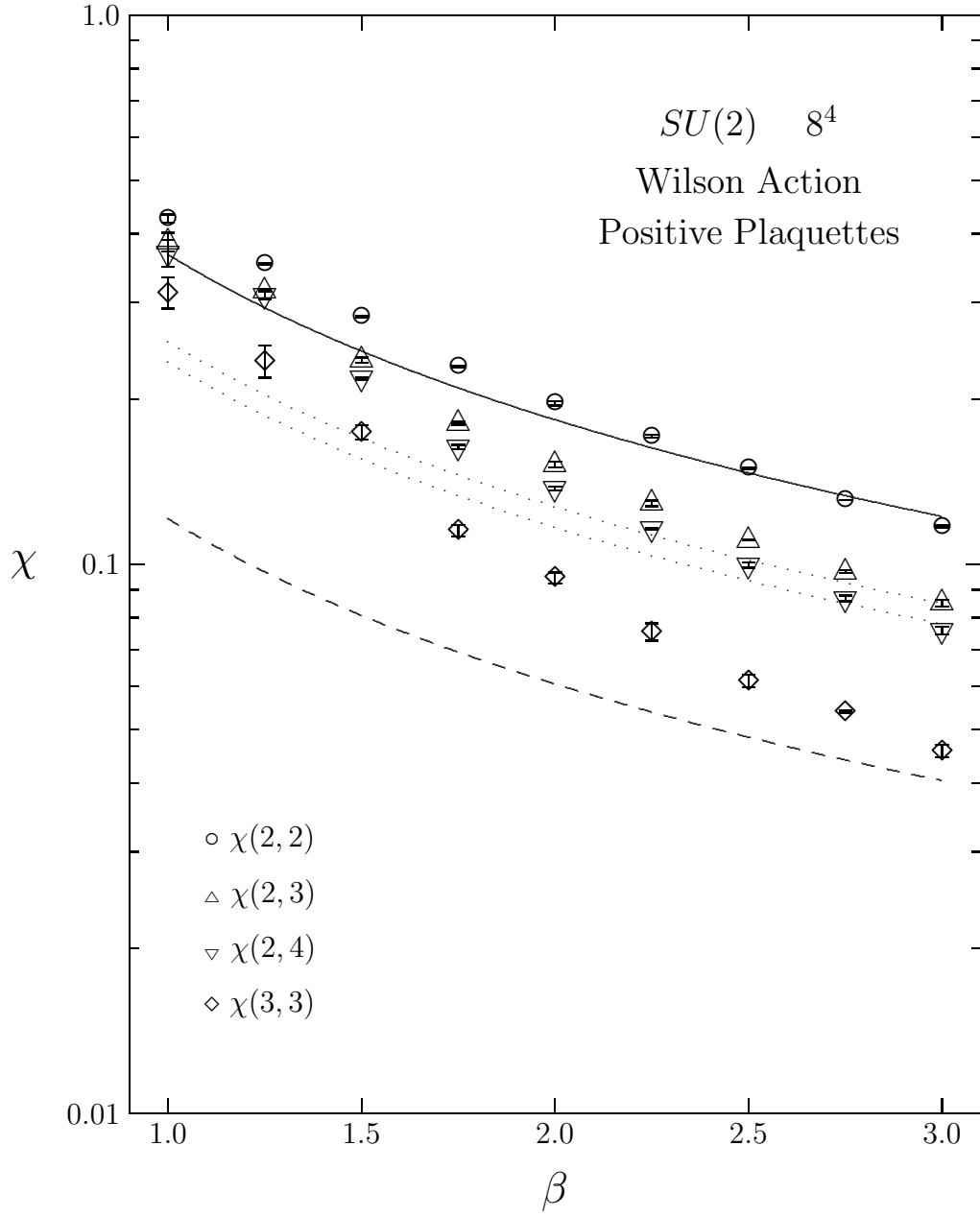


Figure 3: The $SU(2)$ Creutz ratios $\chi(i, j)$ as given by Wilson's action restricted to positive plaquettes and the tree-level perturbative formula $\chi_0(i, j, \beta_e)$ for the Creutz ratios $\chi(2, 2)$ (solid), $\chi(2, 3)$ (dots), $\chi(2, 4)$ (dots), and $\chi(3, 3)$ (dashes) at the effective inverse coupling $\beta_e = 0.54 \beta$.

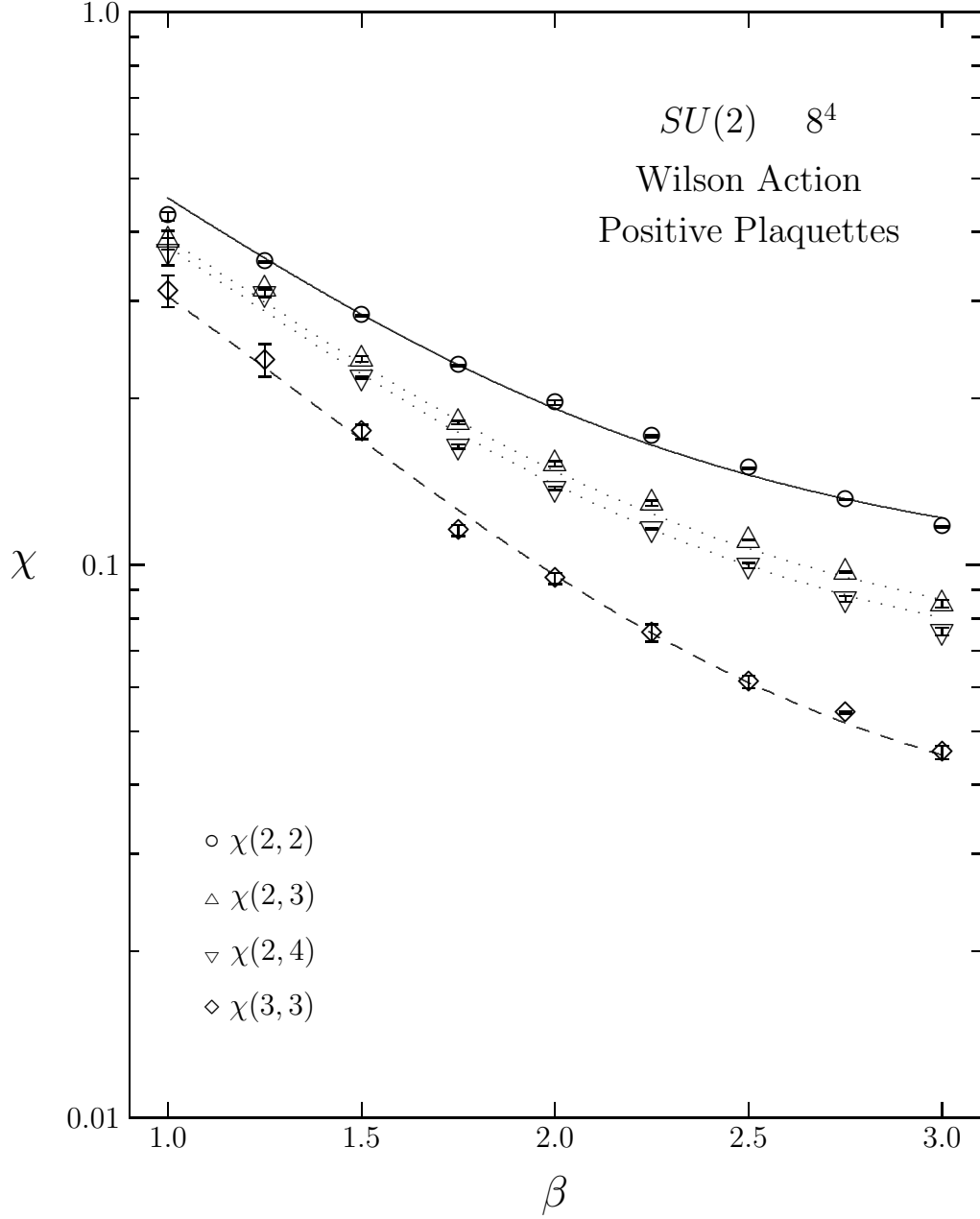


Figure 4: The $SU(2)$ Creutz ratios $\chi(i, j)$ as given by Wilson's action restricted to positive plaquettes and the fit (9) to the Creutz ratios $\chi(2, 2)$ (solid), $\chi(2, 3)$ (dots), $\chi(2, 4)$ (dots), and $\chi(3, 3)$ (dashes).

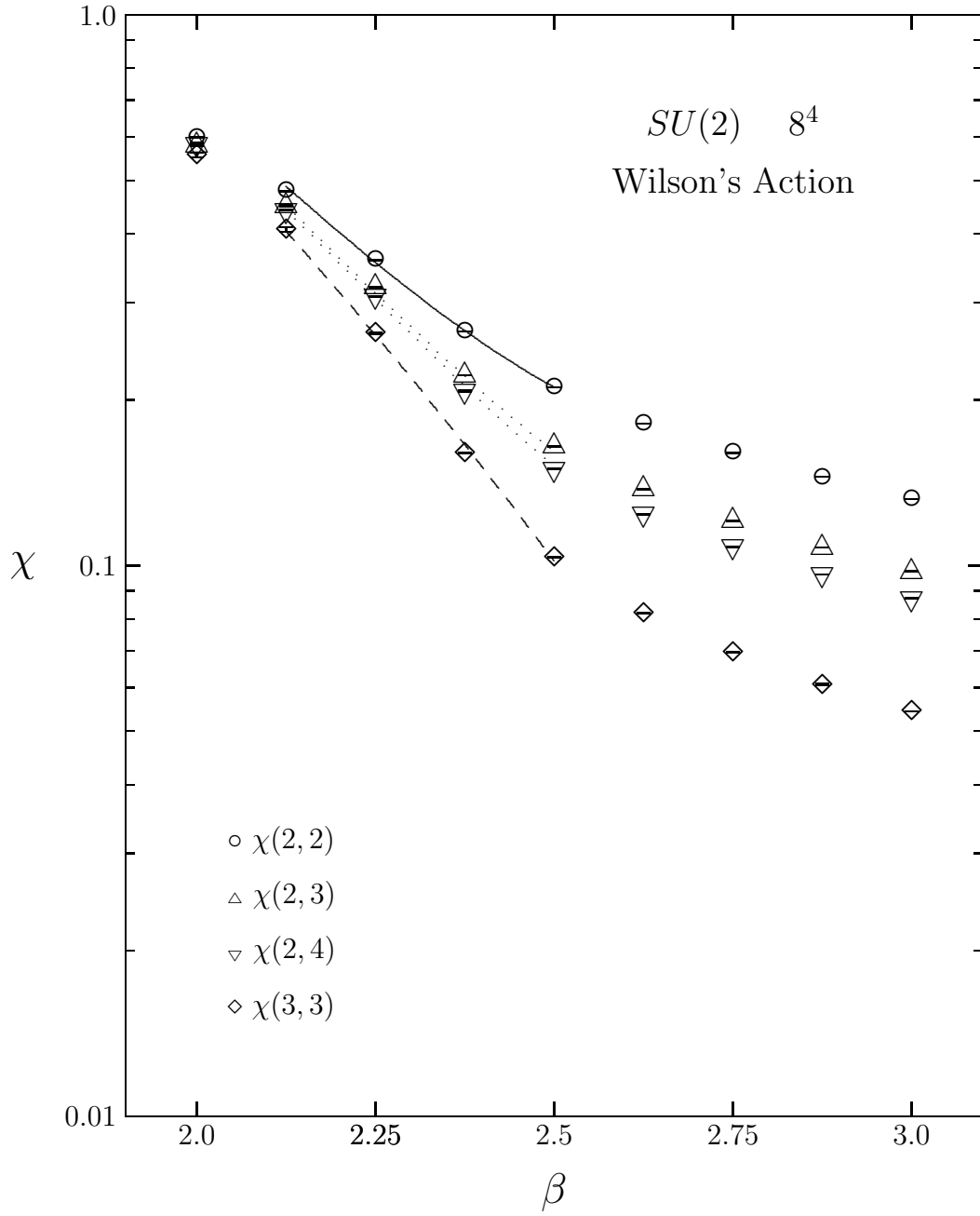


Figure 5: The $SU(2)$ Creutz ratios $\chi(i, j)$ as given by the unmodified Wilson action and the fit (9) to the Creutz ratios $\chi(2, 2)$ (solid), $\chi(2, 3)$ (dots), $\chi(2, 4)$ (dots), and $\chi(3, 3)$ (dashes) between $\beta = 2.125$ and $\beta = 2.5$.